Cite this article: LV Y B, TIAN X L, LI X, et al. Two-dimensional numerical simulation of NACA 0012 flapping foil hydrodynamics[J/OL]. Chinese Journal of Ship Research, 2018, 13(2). http://www.ship-research.com/EN/Y2018/V13/I2/7. DOI: 10.3969/j.issn.1673-3185.2018.02.002.

Two-dimensional numerical simulation of NACA 0012 flapping foil hydrodynamics

LV Yuanbo[1,2], *TIAN Xinliang*[1,2], *LI Xin*[1,2], *SONG Chunhui*[1,2]

1 State Key Laboratory of Ocean Engineering, Shanghai Jiao Tong University, Shanghai 200240, China

2 Collaborative Innovation Center for Advanced Ship and Deep-Sea Exploration, Shanghai 200240, China

Abstract: [**Objectives**] In order to study the impact of the hydrodynamic performance of foil in the design of a wave glider, [**Methods**] on account of the characteristics of the oscillating foil when the wave glider is heaving, and based on the Dynamic Fluid Body Interaction (DFBI) module in STAR-CCM+ with the SST k-ω turbulence model, the passive oscillating process of foil when it is forced to heave is simulated. The effects of limit angles, wave heights and frequencies on the thrust coefficient of NACA 0012 flapping foil are investigated. [**Results**] We find that the passive rotation method can effectively simulate foil oscillating process, and its thrust coefficient is about 30% smaller than the coefficient obtained by the active rotation method. Moreover, the maximum limit angle of a wave glider of around 20° gives a better hydrodynamic performance. The numerical simulation result indicate that the thrust coefficient increases with the increase of wave height and wave frequency in a certain region. [**Conclusions**] This can provide a reference for propulsive performance and hydrodynamic performance under different states of the sea.

Key words: wave glider; passive oscillating; limit angle; propulsive performance

CLC number: U661.3

0 Introduction

Since Hine et al.[1] pioneered the development of a wave glider, as a marine device that directly converts wave energy into forward kinetic energy, wave gliders are widely used in long-term observation operations at sea. Because of its strong endurance, low noise and other advantages[2-3], wave glider has broad application prospects in the detection of marine environmental factors, marine disaster prediction and marine scientific research.

The foil is an important factor influencing the navigation performance of a wave glider, so scholars in the world have conducted a lot of research on the hydrodynamic performance of foil. Kraus[4] established a model to simulate the six-degrees-of-freedom of various parts of the wave glider, indicating that the performance was best when the oscillating angle of the foil was 20°, and the hydrodynamic parameters of the glider under different sea conditions were obtained through simulation. Jia[5] used FLUENT software to study the influence of airfoil profile and oscillating angle on the hydrodynamic characteristics of the foil and found that the hydrodynamic performance was better when the oscillating angle was 18°. Sun et al.[6] carried out numerical simulation on the active oscillation of the wings of fruit flies and it was found that the dynamic average lift coefficient could reach twice the quasi-static lift coefficient. Andersen et al.[7] performed numerical and experimental

Received: 2017-06-12

Supported by: National Natural Science Foundation of China (51509152, 11632011)

Author(s): LV Yuanbo, male, born in 1993, master candidate. Research interest: hydrodynamic analysis of wave glider. E-mail: 15821168683@163.com

TIAN Xinliang (Corresponding author), male, born in 1986, Ph. D., lecturer. Research interest: fluid dynamics, monitoring and control of marine engineering device. E-mail: tianxinliang@sjtu.edu.cn

LI Xin, female, born in 1975, Ph. D., associate professor. Research interest: hydrodynamic performance of offshore platforms and mooring systems. E-mail: lixin@sjtu.edu.cn

SONG Chunhui, male, born in 1993, master degree candidate. Research interest: hydroelasticity. E-mail: chunhui.song@sjtu.edu.cn

studies on active oscillating and active heaving oscillation of a symmetric airfoil. It was found that the wake flow fields of the two kinds of motion models were similar, but for the heaving oscillation at low frequency and high amplitude, two pairs of symmetrical wake vortices were generated within one oscillation period. Hu [8] calculated the entire glider and the foil section by means of a combination of potential flow and viscous flow, and obtained the optimal oscillating angle of the foil at around 15°. Zhang et al. [9] and Liu et al. [10] used the Computational Fluid Dynamics (CFD) software to simulate the unsteady hydrodynamic performance of a two-dimensional rigid foil oscillation according to the principle of oscillating fish tail fin.

In this paper, NACA 0012 is chosen as the airfoil of gliders. For this airfoil, Ohtake et al. [11] and Yonemoto et al. [12] conducted extensive research and obtained the performance parameters of the wing under steady flow field. Read et al. [13] and Triantafyllou et al. [14] conducted experiments with a set of foil active oscillation devices and analyzed the hydrodynamic performance of the NACA 0012 foil under active oscillation and heaving oscillation. It was concluded that unsmooth changes in the effective angle of attack would degrade the foil performance. Schouveiler et al. [15], through the heaving oscillation and active oscillation of the NACA 0012 airfoil following the sinusoidal law, obtained the conclusion that the Strouhal number *St* of the best propulsion efficiency was 0.25-0.35 and the hydrodynamic performance decreased when *St* was large in the test at the MIT towing pool. Because the wing of a wave glider has a passive rotation caused by heaving oscillation, the actual motion of the wing simulated by the active motion of the foil may have large errors. In the passive rotation, it is necessary to consider the transient coupling between the oscillation of the foil and the movement of the flow field. It is also important to consider the constraints imposed by the torque and the limit angle of the foil movement in the flow field. Although there is some difficulty in simulation, it is better for the foil oscillation process. However, studies on the passive oscillation of foil in unsteady flow field are rarely involved at present.

In this paper, based on the Dynamic Fluid Body Interaction (DFBI) module in STAR-CCM + software and taking the NACA 0012 airfoil as the research object, the passive rotation around its own central axis caused by the heaving oscillation of the wave glider's foil is simulated. The thrust coefficient of foil active rotation and passive rotation are compared, and the influence of limit angle and wave parameters on foil performance is analyzed, so as to provide reference for the design and research of wave gliders.

1 Theoretical overview

1.1 Motion theory of a wave glider

The motion theory of a wave glider is shown in Fig.1(a) [16]. A wave glider is composed of a surface mother ship and an underwater glider. When the surface mother ship rises with the waves, the cables will be pulled tightly to drive the underwater glider upward and the glider's foil will flip counterclockwise due to the force of water. When the surface mother ship descends with the wave, the cables loose, and the water glider slides down freely. The foil oscillates clockwise due to the counterforce of water. Constant up and down oscillations will generate forward thrusts, dragging the mother ship to continue to advance.

Fig.1(b) shows the results of the stress analysis of the foil during wave fluctuations. As the foil ascends with the wave, it is subjected to a downward hydrodynamic action perpendicular to the wing surface, which produces a horizontal component F_x and a vertical component F_y. While descending with the waves, the foil is subjected to an upward hydrodynamic action perpendicular to the wing surface, which also produces a horizontal component F_x and a vertical component F_y. During the process, the horizontal component force F_x is the propulsive force to move the wave glider forward. As shown in

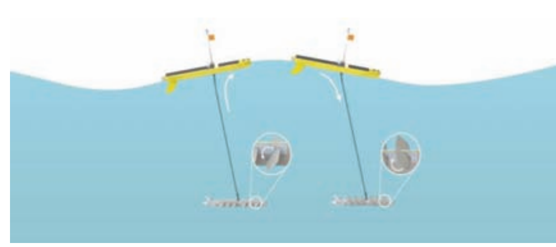

(a) Motion diagram of the wave glider

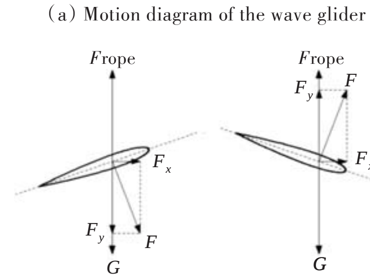

(b) Force analysis of the foil

Fig.1 The motion theory of the wave glider

Fig.1(b), the entire research object is simplified as the foil model.

1.2 Passive motion equation of foil

The movement of the wave glider's foil is divided into two parts: one is the translational motion in the y -direction driven by the wave; the other is the pendulum motion affected by the hydrodynamic force during translation.

The vertical motion of the foil $h(t)$ is

$$h(t)=h_0\sin(2\pi ft) \tag{1}$$

where t is motion time; f is motion frequency; h_0 is the vertical motion amplitude.

The passive motion equation of foil pendulum is

$$J\ddot{\theta}=M(t) \tag{2}$$

where J is the moment of inertia around the center of gravity; $\ddot{\theta}$ is the angular acceleration of the foil's passive rotation; M is the hydrodynamic moment acting on the foil which can be obtained from the pressure integral of foil surface. After integrating Equation (2), the angular velocity $\dot{\theta}$ and the oscillating angle θ can be obtained.

While designing the foil of a wave glider, when the oscillating angle θ of the foil reaches the limit angle θ_0, the oscillating angle reaches its maximum value until the torque is reversed, and the foil starts to oscillate in the opposite direction, which is

$$-\theta_0\leqslant\theta\leqslant\theta_0 \tag{3}$$

1.3 Active motion equation of foil

For the foil oscillation, if the active motion model is adopted in both the vertical direction and the oscillating direction, the motion law of the oscillating direction is

$$\theta(t)=\theta_0\sin(2\pi ft-\psi) \tag{4}$$

where ψ is the phase difference between translational motion and oscillating motion.

For active rotation, the effective angle of attack $\alpha(t)$ is the actual attack angle formed between the combined velocity of the horizontal flow velocity and translation velocity and the oscillating angle of the foil, which can be expressed as

$$\alpha(t)=\theta(t)-\text{arc tan}\left[\frac{h'(t)}{U}\right] \tag{5}$$

where $h'(t)$ is the translational speed; U is the inflow velocity, i.e., the advance velocity of the foil.

Here, the similarity Strouhal number St in fluid mechanics is introduced:

$$St=fA/U \tag{6}$$

where A is the width of wake vortex in the translational direction, which is approximately expressed as two times the translational amplitude, namely $A=2h_0$. After substituting it into Equation (6), the result is $St=2fh_0/U$. Combining with Equation (5), there is

$$\theta_0=\text{arc tan}(\pi St)-\alpha_{\max} \tag{7}$$

where $\alpha_{\max}$ is the maximum effective angle of attack.

1.4 Thrust coefficient

The instantaneous thrust coefficient of foil is

$$C(t)=F_x(t)/\left(\frac{1}{2}\rho bsU^2\right) \tag{8}$$

where $F_x(t)$ is the instantaneous thrust of the foil; ρ is the density of water; b is the chord length of the foil; s is the span of the foil.

The average thrust

$\bar{F}_x$ of a foil in a cycle is defined as

$$\bar{F}_x=\frac{1}{T}\int_0^T F_x(t)\mathrm{d}t \tag{9}$$

where T is the rotation period of the foil.

The average thrust coefficient is

$$\bar{C}(t)=\bar{F}_x/\left(\frac{1}{2}\rho bsU^2\right) \tag{10}$$

2 Numerical model and verification

2.1 Model parameters

The foil adopts the NACA 0012 airfoil where the maximum thickness is located at 1/3 of the chord length, as shown in Fig.2. The characteristic chord length of the foil is b=0.1 m and the oscillating axis is located at the spot with the maximum thickness.

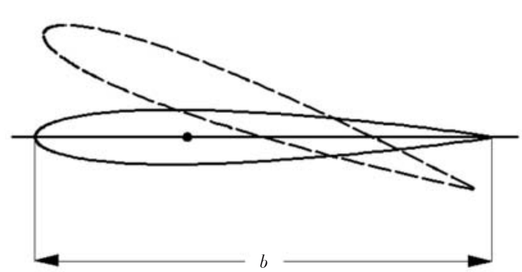

Fig.2 Hydrofoil profile of NACA 0012

2.2 Numerical model

As shown in Fig.3, the computational domain of the two-dimensional oscillating foil is $50b\times30b$. The surface is a circular calculation domain with a diameter of $5b$ for the rotating motion of the wing. For the boundary conditions, the left border, the upper and lower borders are the speed inlets and the right border is the pressure exit.

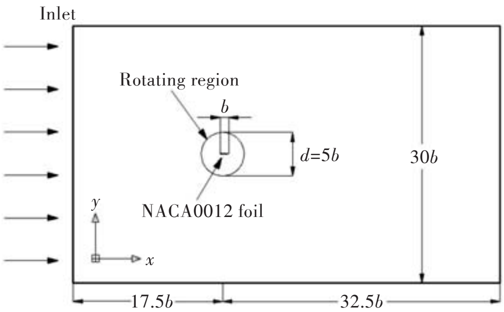

Fig.3 Computational domain and boundary conditions

The SST k-ω turbulence model is used for the calculation and the watershed is segmented using the mesh of the STAR-CCM + software. As shown in Fig.4, on the surface of the foil, an overset mesh with no relative deformation and good numerical exchange is used and local encryption in the computational domain and wake flow area is performed. The boundary has 30 layers and $y+$ is controlled strictly less than 1. As for the foil motion, the DFBI module in STAR-CCM+ software is used to simulate the undulating process by inputting the sinusoidal boundary conditions of the upper and lower surface boundaries. Then, the DFBI module calculates the passive rotation of the foil under heaving oscillation and controls the maximum angle of rotation of the foil, namely the limit angle θ_0, through the single-degree-of-freedom rotation module.

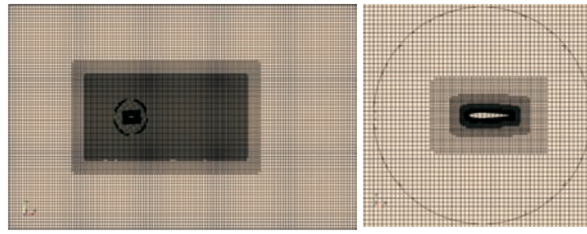

(a) Mesh scheme of the whole computational domain

(b) Mesh scheme of the wing surface

Fig.4 Mesh scheme

2.3 Numerical model validation

In order to validate whether the established numerical model satisfies the calculation requirements, it is necessary to verify the mesh size, time step and reliability of the calculation results.

2.3.1 Validation of mesh size

In order to ensure the accuracy and efficiency of the calculation, the lifting coefficients C_L at the fixed angles of the four mesh sizes are calculated, analyzed and compared. Table 1 shows the values of C_L and relative errors (between the calculated and experimental values) corresponding to the four mesh sizes A1-A4 at a fixed angle of 5°. It can be observed that the calculated value tends to be stable from A2. According to the empirical analysis of the airfoil, the C_L experimental value is generally slightly less than the CFD calculated value. It can be observed that the calculated value is very close to the theoretical value.

Table 1 The mesh size validation

Mesh size	Number of meshes	Number of overset meshes	Number of background	Predicted C_L	Theoretical value of C_L	Experimental value of C_L	Relative error/%
A1	221 574	180 401	41 173	0.535 078	0.548 311	0.511	2.47
A2	483 439	414 619	68 820	0.546 092	0.548 311	0.511	0.41
A3	654 312	563 258	91 054	0.546 114	0.548 311	0.511	0.40
A4	905 687	783 720	121 967	0.546 114	0.548 311	0.511	0.40

Fig.5 shows the pressure coefficient C_p distribution of the upper and lower wing surfaces with four mesh sizes. It can be observed that: A2, A3 and A4 all coincide well. A1 fluctuates at about 1/3 of the upper surface. Combining with the flow field in this area, it is found that boundary layer has a clear separation. The mesh size of A1 boundary layer is large and cannot be accurately captured. Considering the calculation amount and accuracy, A2 is selected as the grid model.

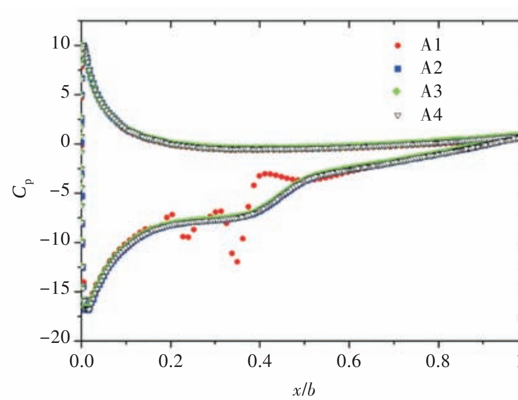

Fig.5 The pressure coefficient distribution of the wing surface with different meshes

2.3.2 Validation of time step

Under the A2 model, the active heaving oscillation is applied to the foil to superimpose the rotation around the center through the Motion module in the STAR-CCM + software. The peak lift coefficient $C_{L\max}$ (Table 2) is calculated taking the time steps

Δt as T_0/100, T_0/200, T_0/300 and T_0/400, respectively. As can be seen from Table 2, in addition to the time step of T_0/100, the $C_{L\max}$ of other conditions are close.

Table 2 Time step validation of A2

Number of meshes	Number of overset meshes	Number of background	$\Delta t/T_0$	$C_{L\max}$
483 439	12 040	37 236	1/100	2.228 72
483 439	24 357	37 236	1/200	2.301 94
483 439	28 916	122 490	1/300	2.310 18
483 439	28 916	141 846	1/400	2.330 72

Fig.6 shows the relationship between lift coefficient C_L and time T under different time steps. Compared with other time steps, T_0/100 shows a large phase deviation at the peak fluctuation and the number of peaks decreases. Considering the amount of calculation and the accuracy of calculation, $\Delta t/T_0$ =1/200 is chosen as the time step of the model.

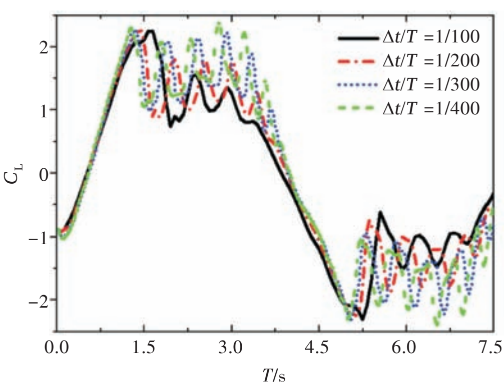

Fig.6 The lift coefficient curve of active rotary motion under different time step

2.3.3 Reliability validation

In order to verify the accuracy of the model, the calculated values are compared with the two experimental values in Reference [12] with the same fixed oscillation angle and Reynolds number. The angle of attack α is chosen at every 1° between −5°−+5° and Re= 10^5. Fig.7 shows the lift and drag coefficients of the foil at a fixed oscillation angle. Fig.7(a) shows that the calculated values agree well with the experimental values, and C_L shows higher accuracy and broader data range than Yonemoto's calculated value. Moreover, the straight line in Fig.7(a) is the theoretical value with the slope a=2π. It can be seen from Fig.7(b) that both the drag coefficient C_D and the Yonemoto calculation results are slightly lower than the experimental values and the calculation results are basically consistent. Therefore, the numerical model can be used to accurately calculate the hydrodynamic characteristics of foil.

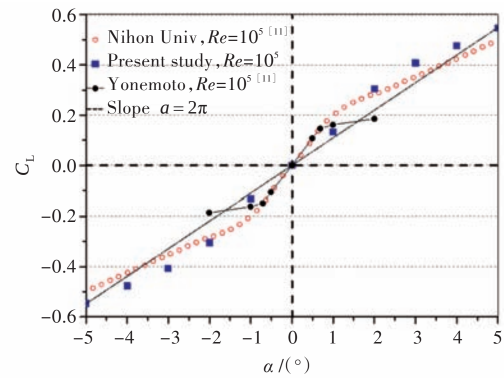

(a) The lift coefficient of the wing

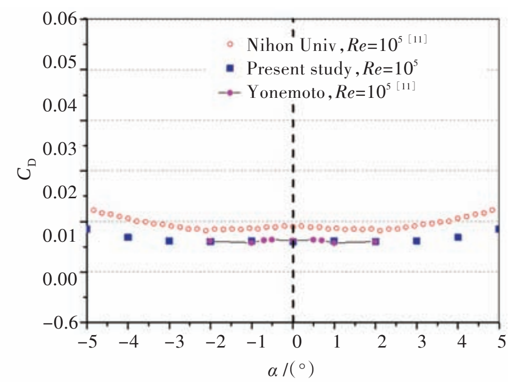

(b) The drag coefficient of the wing

Fig.7 The lift and drag coefficients of the wing with fixed angular

3 Calculation results and analysis

For active and passive rotations of foil, the hydrodynamic performance is simulated in STAR-CCM+ software. The simulation results are compared and the effects of limit angles, wave heights and frequencies on the thrust coefficient are emphasized. The conditions for active and passive rotations are shown in Table 3 and Table 4, respectively.

Table 3 The calculation conditions for active oscillating wing

Parameter	Value	Parameter	Value
U/(m·s^{-1})	0.4	St	0.1~0.6
α_{max} /(°)	15	Re	4×10^4
h_0 /m	0.1, 0.4, 0.8	ψ /(°)	90
f/Hz	0.1~1.2		

Table 4 The calculation conditions for passive oscillating wing

Parameter	Value	Parameter	Value
U/ (m·s^{-1})	0.4	f/Hz	0.1~1.2
θ_0 /(°)	10, 15, 20, 25, 30	Re	4×10^4
h_0 /m	0.1, 0.4, 0.8, 0.9, 1.0		

3.1 Influence of active and passive rotations on propulsive performance

In order to compare the influence of active and passive rotations on propulsive performance, inflow speed U=0.4 m/s, the maximum effective angle of attack $\alpha_{max}=15°$ and h_0 =0.8 m are taken to analyze the thrust coefficients of the active and passive oscillating wings under different St, and the results are shown in Fig.8.

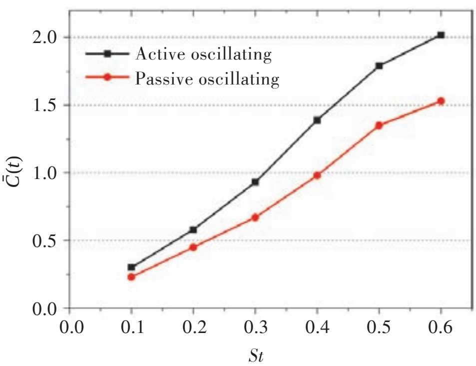

Fig.8 The thrust coefficient curves of the active and passive oscillating wing under different St

It can be seen from Fig.8 that whether it is active oscillation or passive oscillation, the average thrust coefficient of the foil increases with the rise in St in one cycle and the thrust coefficient of active oscillating wing is greater than that of passive one. Moreover, the average thrust coefficient obtained by active oscillation method is about 30% higher than the coefficient obtained by the passive rotation method. This is mainly because of the different rotation speeds of the two. When simulating with the passive rotation method, the foil instantaneously flips when it rises or falls due to the reaction force of water, and the rotation speed reaches the maximum at that moment. The rotation speed reduces to 0 when the limit angle reaches the maximum, and then the foil performs translational movement with this limit angle. However, the traditional active rotation method is different. The foil has a given sinusoidal oscillating rate rotates at the fastest speed near the equilibrium position. During the process from the equilibrium position to the wave peak, instead of instantaneously completing the flip, the foil periodically oscillates at a sinusoidal rate which generates an additional thrust backwards to the water, thus allowing the foil to gain additional forward propulsive force, increasing the average thrust coefficient. From the perspective of energy, the input energy of the passive oscillating wing is only the energy required for the heaving oscillation, while the input energy of the active oscillating wing is the sum of the energy required for the active heaving oscillation and the active rotation. Therefore, compared with the passive oscillation, the energy of the active rotation is greater, thus producing greater thrust.

Fig.8 also shows that when St is small, the difference in the average thrust coefficients between the two is small. With the gradual increase in St, the difference between the two gradually increases and tends to be stable, which can reach 30%. It is clear that the active and passive rotations have a great influence on the propulsive performance. For the hydrodynamic performance of wave glider foil, the traditional active oscillation model increases the calculation error and cannot accurately simulate the actual motion of wave glider foil.

3.2 Influence of limit angle θ on propulsion performance

Five limit angles are selected for the study of the influence of limit angle θ on propulsion performance. The other parameters are set as follows: inflow velocity U=0.4 m/s, wave frequency f=0.2 Hz and wave height h=0.8 m. The thrust coefficient curves are shown in Fig.9.

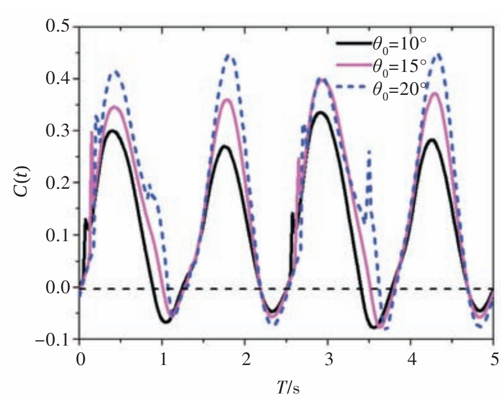

(a) Comparison of $C(t)-T$ curve under 10° to 20°

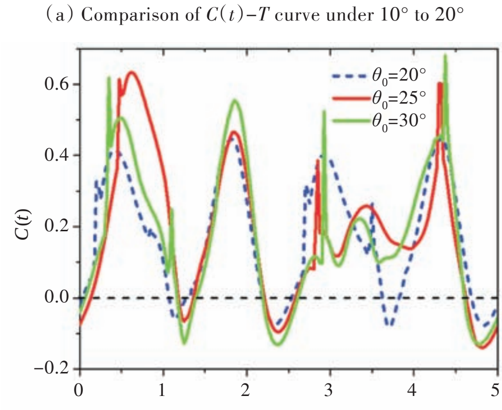

(b) Comparison of $C(t)-T$ curve under 20° to 30°

Fig.9 The thrust coefficient curves of the passive oscillating wing under different limit angles

From Fig.9(a), it can be analyzed that when the maximum limit angles of the passive oscillating oscillation θ_0 are at 10°, 15° and 20°, the thrust coefficient $C(t)$ makes a periodic sine-like change with time and gradually increases as the maximum limit angle increases. At the limit angle $\theta_0 = 20°$, the peak value of the thrust coefficient reaches the maximum.

Fig.9(b) shows the $C(t)$–T curve under the maximum limit angles of the passive oscillation θ_0 at 20°, 25° and 30°. It can be seen that in the first half cycle, the peak value of the thrust coefficient increases with the rise in the limit angle. However, in the latter half, the peak of $C(t)$ appears abrupt change and cuspidal point at the limit angles of $\theta_0 = 25°$ and $\theta_0 = 30°$, which fails to present a good periodicity. The reason for the abrupt change is that when the oscillating angle is greater than 25°, the foil starts to stall gradually due to the interaction between the distant inflow and the flow separation of upper surface of the foil, which has a significant impact on thrust performance. Therefore, when the oscillating angle exceeds a certain critical value, the thrust coefficient will stop rising and significant fluctuations will appear.

Fig.10 shows the vorticity contours of the passive oscillating wing at $T/4$ under different limit angles. It can be seen from the vorticity contours that under the limit angle $\theta_0 = 10°$–$20°$, the upper surface of foil has a small separation area and presents with a streamlined flow. However, as oscillating the angle gradually increases from 25°, the trailing edge of the foil produces a pronounced vortex, and the separation area on the upper surface of the airfoil gradually increases. Moreover, the wingtip vortex begins to form near the trailing edge, which reduces the hydrodynamic performance of foil to a certain extent. As shown in Fig.10, the shedding vortices of the foil are all in the form of a comma. The jet generated at the tail increases the thrust of the foil. As the limit angle increases, the size of the shedding vortices gradually decreases.

Based on the above analysis, $\theta_0 = 20°$ is selected as the maximum limit angle of the passive oscillating wing.

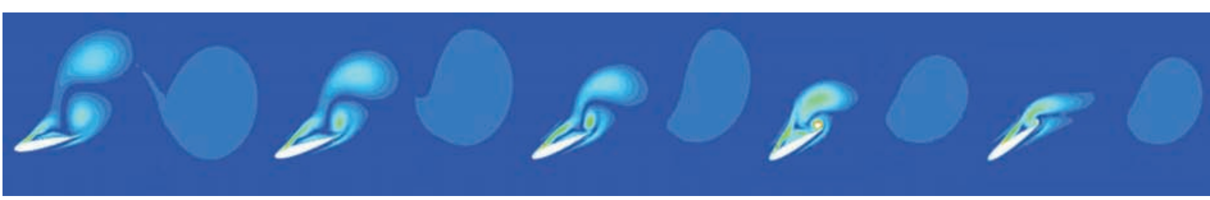

(a) $\theta = 10°$ (b) $\theta = 15°$ (c) $\theta = 20°$ (d) $\theta = 25°$ (e) $\theta = 30°$

Fig. 10 The vorticity contours of the passive oscillating wing under different limit angles

3.3 Influence of wave height h and wave frequency f on the propulsion performance of foil

The limit angle $\theta = 20°$ has been determined. When the inflow velocity U=0.4 m/s and wave frequency f=0.2 Hz, three wave heights h= 0.1, 0.4 and 0.8 m are selected, and the corresponding curves $C(t)$–T of passive oscillating wing under different wave heights are obtained (as shown in Fig.11).

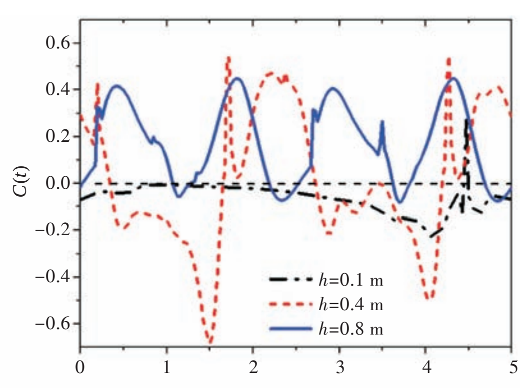

Fig.11 The $C(t)$–T curves of the passive oscillating wing under different wave heights with f=0.2 Hz

It can be seen from Fig.11 that $C(t)$ increases with increasing wave height h. The thrust coefficient curve shows no obvious periodicity and most of $C(t)$ is less than 0 at wave heights h=0.1 m and h=0.4 m, which indicates that the flow field does not tend to be stable. When h=0.8 m, the curve begins to show obvious periodicity. In addition, with the wave frequency f=0.2 Hz, the thrust coefficient increases gradually with the rise in wave height h. Moreover, at a certain inflow velocity and wave frequency, the wave height needs to reach a certain height to produce stable forward thrust, and the flow field and the thrust coefficient also tend to be stable.

The above discussion on the wave height h is limited to a single frequency, i.e., f=0.2 Hz, so the law is not universal. To find out the influence of the wave height h on the propulsion performance of foil, multiple sets of working conditions are selected and the calculation results are compared.

The wave height h is determined to be around 0.8 m as the thrust coefficient shows periodicity when h= 0.8 m and the wave frequencies f=0.1, 0.2 and 0.4 Hz are selected to study the effect of different wave heights h on $C(t)$ (as shown in Fig.12). As can be seen from Fig.12, under different wave frequencies, the thrust coefficient $C(t)$ increases with the rise in wave height h.

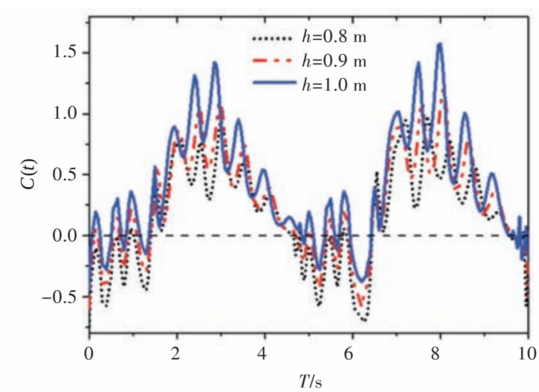

(a) Wave heights influence under f=0.1 Hz

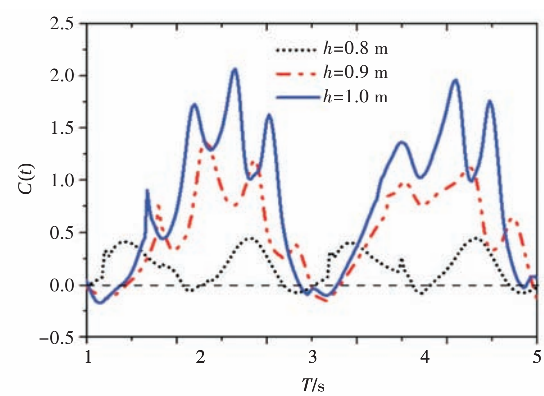

(b) Wave heights influence under f=0.2 Hz

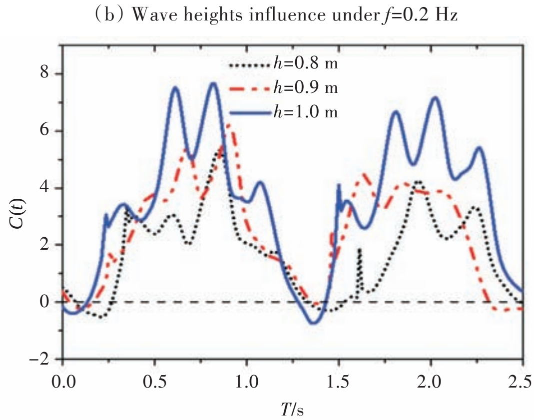

(c) Wave heights influence under f=0.4 Hz

Fig.12 The $C(t)$−T curves of the passive oscillating wing under different wave heights

From the above calculation results, it can be seen that the thrust coefficient $C(t)$ tends to be stable starting from the wave height h=0.8 m when other conditions are constant. Therefore, different wave frequencies are selected when the wave height h=0.8 m and the inflow velocity U=0.4 m/s.

Fig.13 shows $C(t)$−T curve of the passive oscillating wing under different wave frequencies with h= 0.8 m. It can be seen from the figure that when wave frequency f= 0.2 Hz, the thrust coefficient fluctuates at around $C(t)$ = 0. For every doubling of the wave frequency f, the increase in $C(t)$ is much higher than double. When f=0.8 Hz, the peak of $C(t)$ reaches 20. It can be seen that the influence of wave frequency f on the thrust coefficient $C(t)$ is more significant. In short, the thrust coefficient $C(t)$ increases with the rise in the wave frequency f with h = 0.8 m.

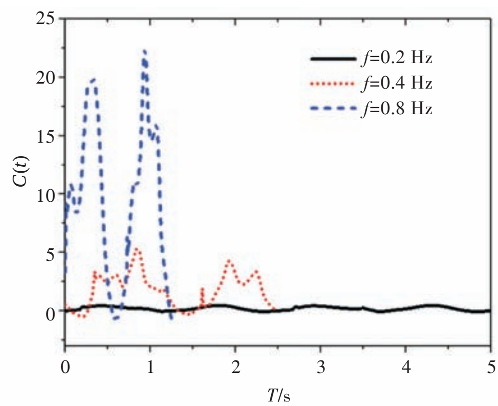

Fig.13 The $C(t)$−T curve of the passive oscillating wing under different wave frequencies with h=0.8 m

Similarly, the above discussion of wave frequency is also limited to a single wave height, namely h= 0.8 m, which is not universal. To further study the influence of the wave frequency f on the propulsion performance of foil, multiple sets of working conditions are selected and the calculation results are compared, respectively.

Fig.14 shows the effect of different wave frequencies f on $C(t)$, from which it can be seen that at different wave heights, the thrust coefficient $C(t)$ increases with the rise in the frequency f. When the wave frequency increases from 0.2 Hz to 0.4 Hz, the peak of $C(t)$ curve is increased by 5−10 times. However, when the wave frequency is low, namely f=0.1 Hz and f=0.2 Hz, the peak value of the thrust coefficient $C(t)$ changes very little. Therefore, when the wave frequency is small, the change of the wave frequency f has a little effect on the thrust coefficient.

4 Conclusions

In this paper, taking the underwater foil of a wave glider as the research object, the hydrodynamic analysis and calculation of the passive oscillation of NACA 0012 foil in waves are carried out. The following main conclusions are obtained:

1) Through the model that combines the DFBI

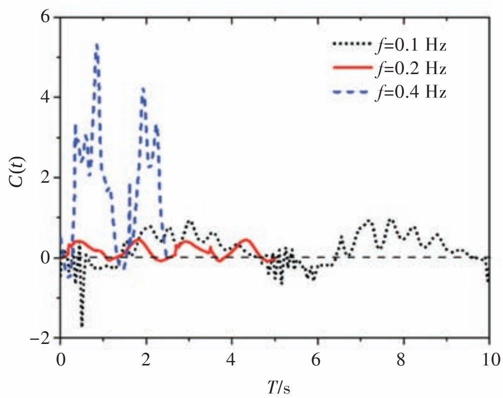

(a) Wave frequency influence under h=0.8 m

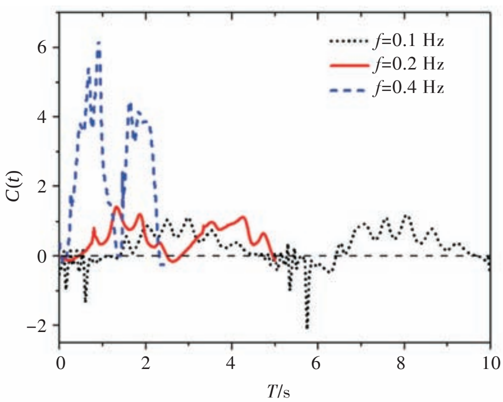

(b) Wave frequency influence under h=0.9 m

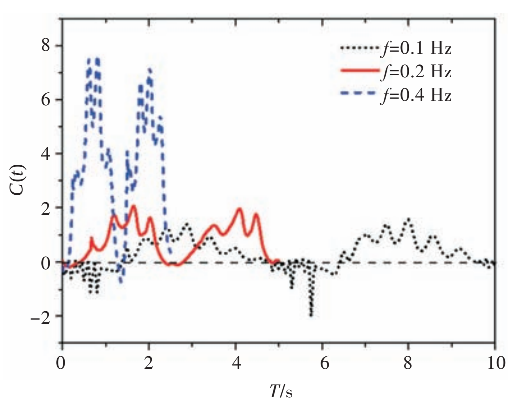

(c) Wave frequency influence under h=1.0 m

Fig.14 The $C(t)-T$ curve of the passive oscillating wing under different wave frequencies

module and independently built overset mesh in the STAR-CCM+ software, the passive rotation simulation of the foil in the vertical translation state is realized.

2) Under the same condition, the active and passive oscillations have a great influence on the propulsive performance of soil, and the difference of average thrust coefficient of the two can reach 30%.

3) By analyzing the calculation results and the vorticity contours, it is found that the hydrodynamic performance of the glider is optimal when the maximum limit angle of the foil is around 20°.

4) When other conditions are fixed, the propulsion performance of the foil is greatly affected by the wave parameters, which is increased with the rise in wave height h and wave frequency f. When the frequency is small, the change of wave frequency f has a little effect on the thrust coefficient.

References

[1] HINE R, WILLCOX S, HINE G, et al. The wave glider: a wave-powered autonomous marine vehicle[C]// OCEANS 2009, MTS/IEEE Biloxi-Marine Technology for Our Future: Global and Local Challenges. Mississippi: IEEE, 2009: 1-6.

[2] XU C Y, CHEN J W, ZHENG B H. Research status and applications of wave gliders[J]. Journal of Ocean Technology, 2014, 33(2): 111-117 (in Chinese).

[3] YANG H, LIU Y J, ZHANG K. Design and experiment for laboratory-scale autonomous underwater gliders[J]. Chinese Journal of Ship Research, 2016, 11 (1):102-107,120 (in Chinese).

[4] KRAUS N D. Wave glider dynamic modeling parameter identification and simulation[D]. Hawaii: University of Hawaii, 2012.

[5] JIA L J. Study of operation principal of two-part architecture and dynamic behavior of wave glider[D]. Tianjin: National Ocean Technology Center, 2014 (in Chinese).

[6] SUN M, TANG J. Unsteady aerodynamic force generation by a model fruit fly wing in flapping motion[J]. Journal of Experimental Biology, 2002, 205(1): 55-70.

[7] ANDERSEN A, BOHR T, SCHNIPPER T, et al. Wake structure and thrust generation of a flapping foil in two-dimensional flow[J]. Journal of Fluid Mechanics, 2017, 812: R4-1-R4-12.

[8] HU H W. Hydrodynamic analysis of wave glider[D]. Harbin: Harbin Engineering University, 2015 (in Chinese).

[9] ZHANG X Q, WANG Z D, ZHANG Z S. Hydrodynamic study of bionic propulsion for 2D flapping foil[J]. Journal of Hydrodynamics (Ser. A), 2006, 21(5): 632-639 (in Chinese).

[10] LIU H X, SU Y M, PANG Y J. Effects of the nonsinusoidal oscillating on the hydrodynamic performance of the hydrofoil[J]. Journal of Huazhong University of Science and Technology (Natural Science Edition), 2016(2): 15-20 (in Chinese).

[11] OHTAKE T, NAKAE Y, MOTOHASHI T. Nonlinearity of the aerodynamic characteristics of NACA0012 aerofoil at low Reynolds numbers[J]. Journal of the Japan Society for Aeronautical and Space Sciences, 2007, 55(644): 439-445.

[12] YONEMOTO K, TAKATO K, OCHI H, et al. Kutta condition violation in two-dimensional NACA0012 airfoil at low Reynolds number[C]//26th AIAA Applied Aerodynamics Conference. Hawaii: AIAA, 2008: 6399.

[13] READ D A, HOVER F S, TRIANTAFYLLOU M S. Forces on oscillating foils for propulsion and maneu-

vering[J]. Journal of Fluids and Structures, 2003, 17(1): 163-183.

[14] TRIANTAFYLLOU G S, TRIANTAFYLLOU M S, GROSENBAUGH M A. Optimal thrust development in oscillating foils with application to fish propulsion[J]. Journal of Fluids and Structures, 1993, 7(2): 205-224.

[15] SCHOUVEILER L, HOVER F S, TRIANTAFYLLOU M S. Performance of flapping foil propulsion[J]. Journal of Fluids and Structures, 2005, 20(7): 949-959.

[16] Liquid Robotics. Converting wave motion into propulsion[EB/OL].(2014-09)[2017-06].https://www.liquid-robotics.com/platform/how-it-works/.

NACA 0012摆动水翼水动力特性的二维数值模拟

吕元博[1,2], 田新亮[1,2], 李欣[1,2], 宋春辉[1,2]

1 上海交通大学 海洋工程国家重点实验室,上海 200240

2 高新船舶与深海开发装备协同创新中心,上海 200240

摘　要:[**目的**]为了研究水翼的水动力性能对波浪滑翔机设计的影响,[**方法**]针对波浪滑翔机运动时水翼的摆动特点,基于STAR-CCM+软件的流体与固体相互作用(DFBI)模块,采用SST k-ω湍流模型,模拟出滑翔机水翼在一个周期内主动升沉运动下的被动摆动过程,研究限位角、波高、波浪频率等因素对NACA 0012型水翼的推力系数的影响。[**结果**]仿真结果表明,被动旋转方法可以有效模拟水翼摆动过程,且被动旋转方法所得平均推力系数与主动旋转的相比小30%左右;滑翔机水翼最大限位角在20°附近时,水翼的水动力性能较优;平均推力系数在一定范围内随波高、波浪频率的增加而增大。[**结论**]这一结果可为研究波浪滑翔机的推进性能以及在不同海况条件下的水动力性能提供参考。

关键词: 波浪滑翔机; 被动摆动; 限位角; 推进性能